Boundary-Layer Separation from the Electrode Wall of an MHD Generator

C.C.P. Pian* and W.F.H. Merck†
Eindhoven University of Technology, the Netherlands

The compressible, laminar boundary-layer separation from the finitely segmented electrode wall of an MHD generator has been investigated, using a simplified model in order to obtain a quick physical understanding of the particular influence of the segmentation upon the separation process. Calculations, using an implicit finite-difference scheme, were carried out for a variety of externally imposed conditions, for two different electrical conductivity models, and for different kinds of wall boundary conditions in the solution of the energy equation. Results showed that any variations in the externally imposed parameters which tend to increase the Ohmic heating in the duct, to increase the magnitude of the axial Lorentz force, or to decrease the inertia of the fluid elements in the near-wall region will favor earlier separation. In the cases where the wall temperature is specified a priori, separation was found to be nearly independent of the two electrical conductivity models used in the calculations. Separation is also favored in situations where the duct walls are incapable of conveying away the excess Joule heating in the boundary layers.

Introduction

SINCE the increased interest in MHD power generation in the early sixties, much work has been done to analyze the MHD boundary layers, at both the insulator and the electrode walls. In that period laminar problems were studied by Hale and Kerrebrock,[1] Liubimow,[2] and others, using approximate expressions for the electrical conductivity and Hall parameter. Turbulent effects were taken into account by Lykoudis,[3] Argyropoulos et al.,[4] and Ginzburg and Skurin,[5] whereas Sherman et al,[6] Cott,[7] High and Felderman,[8] and Doss[9] introduced more sophisticated calculations methods and took detailed account of the nonequilbirium ionization and relaxation effects. At the Fifth International MHD Conference in Munich, 1971, consensus was that more attention is needed in the area of boundary-layer separation, especially at the electrode wall. This effect can appear in the supersonic MHD generator with high magnetic interaction and can result in severe degradation of the generator performance.[10] Although the phenomenon of boundary-layer separation is well-known and thoroughly studied in aerodynamics, the subject of separation from the finite-segmented electrode wall has not been as extensively investigated.[10,11] The aim of the present paper is to obtain a qualitative understanding of the influence of various parameters, especially the finite segmentation, upon the separation phenomena. For this purpose computer experiments, using the Patankan-Spalding[12] scheme were performed. The calculations are restricted to the solution of the gasdynamic variables whereas the electromagnetic (EM) variables are specified. Further, no detailed account of the electron species behavior was rendered.

Analysis

The boundary layer under study is shown in Fig. 1, together with the coordinate system that will be used. The working part of the MHD generator starts at the point x_1, 0.1 m downstream of the entrance, and separation occurs at the point x_s. The lengths of the conducting and insulating segments are a and b, respectively.

The simplified model encloses the following assumptions: 1) the flow is two-dimensional, $(\partial/\partial z)=0$; 2) the flow is steady, $(\partial/\partial t)=0$; 3) the fluid is a perfect gas; 4) c_p and P_r are constants; 5) the viscosity coefficient follows the Sutherland's formula; 6) no radiation losses; 7) the thickness of the boundary layer is small compared to the electrode pitch;[6,9] 8) a one temperature fluid is considered; 9) the current density $j_y(x)$ along the electrode is superimposed as

$$j_y = -F(x) = -\left[\exp\left(10\frac{x_2}{a}\right) - 1\right]\sin\left(\frac{\pi x_2}{a}\right) j_y \max/2504 \tag{1}$$

and $j_y=0$ over the insulator (Fig 2). This current distribution approximates the actual distribution closely in regions adjacent to the wall; 10) the electric field along the insulator is superimposed, using

$$E_x = G(x) = E_{x\max}\left(\frac{x_3-b}{b}\right) \tag{2}$$

and $E_x=0$ over the conductor (Fig. 2); 11) the main stream current density is homogeneous such that

$$j_{y\infty} = \frac{-1}{a+b}\int_0^a F(x)\,dx \text{ and } j_{x\infty}=o \tag{3a}$$

whereas

$$E_{x\infty} = \frac{1}{a+b}\int_0^b G(x)\,dx \tag{3b}$$

and 12) the magnetic Reynold's number is small, $Rm \ll 1$.

These assumptions lead to the usual set of gasdynamic equations for the boundary layer and the freestream, with the well-known boundary conditions upon the gas velocity and temperature.[1] It is clear that this analysis does not satisfy the electromagnetic equations exactly. A full solution to the two sets of coupled electromagnetic-gasdynamic equations could be obtained, in principle, by an iterative procedure. This entails solving alternately the electromagnetic problem, described by a nonlinear partial differential equation of the elleptic type (or even hyperbolic), and the gasdynamic problem, described by the boundary-layer equations which are parabolic in nature. Since the present investigation into the behavior of separation is qualitative in nature, such a

Received June 16, 1975; revision received June 4, 1976. The authors gratefully acknowledge helpful discussions with L.H.Th. Rietjens, A. Veefkind, J.H. Blom and L. Vroomen. This work was performed while the first author (C.C.P.P.) was a visiting scientist at the Eindhoven University of Technology.

Index categories: Boundary Layers and Convective Heat Transfer—Laminar; Plasma Dynamics and MHD.

*Visiting scientist.

†Staff member of the Group Direct Energy Conversion, Department of Electrical Engineering.

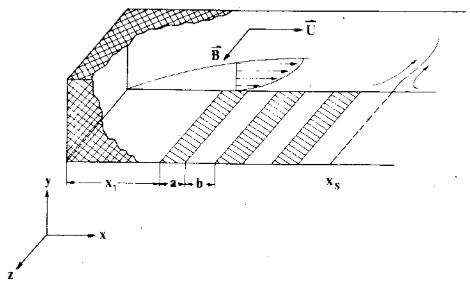

Fig. 1 Geometry and coordinate system.

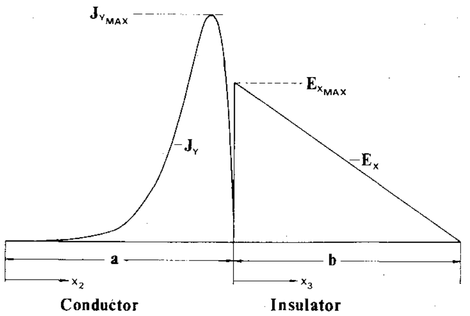

Fig. 2 Imposed current density and electric-field distributions.

detailed and costly procedure is inappropriate. The electromagnetic equations in the boundary layer are thus reduced to the simple form of Ohn's Law

$$j_x = \frac{\sigma}{1+(\omega t)^2}\,[E_x - \omega t(E_y - uB)] \tag{4a}$$

$$j_y = \frac{\sigma}{1+(\omega t)^2}\,[\omega t\,E_x + E_y - uB] \tag{4b}$$

Two models for the electrical conductivity were used, being a constant effective conductivity all over the field and a model that gives account for the nonequilibrium ionization in a certain way, introduced by Hale and Kerrebrock[1]

$$\sigma = \sigma_\infty\left\{\exp\left[-\beta\left(1-\frac{T}{T_\infty}\right)\right]\right\}\,\{(j_x^2+j_y^2)^{1/2}/j_\infty\}^\alpha \tag{5}$$

where α and β are constants.

Method of Solution

The computational scheme used in the present investigation is that of Patankar and Spalding,[12] a modified and improved version of the one that was presented at the Stanford Conference.[13] Results of the predicted separation distances over smooth walls using this newer version compared favorably with experimental data.[14] The general partial differential equations as given by Ref. 12, modified in the present problem to account for the presence of the currents and the magnetic field, are put into an implicit difference form and solved by a marching-intertegration procedure. Variable steps in the streamwise direction are used to enhance the numercial accuracy at the electrode-insulator junctions and over regions of high current concentrations.

The dependent variable profiles used to start the numercial solution of the laminar boundary-layer equations are as follows: the intital velocity distribution is represented approximately by the Pohlhausen one-parameter polynominal profile, while the initial temperature distribution follows the Crocco-Busemann temperature-velocity relationship. The thickness of the boundary layer is taken to correspond to the case of an imaginary sharp leading edge situated 0.1 m upstream of the power section of the duct. Since the assumed initial profiles do not satisfy the conversation equations exactly, sufficient numbers of streamwise calculation steps were taken prior to the first electrode segment to insure that the computer solutions converge to the actual conditions.

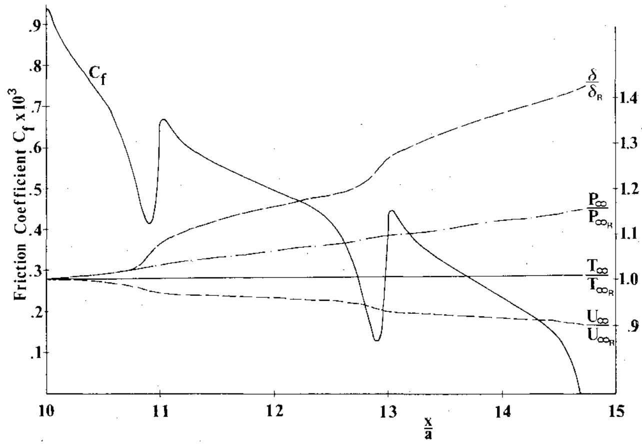

Fig. 3 Variations of friction coefficient, freestream properties and boundary-layer thickness for a typical run with $\delta_R = 1.081\times10^{-3}$m; $P_{\infty R} = 1.5\times10^5$ N/m^2; $T_{\infty R} = 2000$ K; $u_{\infty R} = 1000$ m/sec.

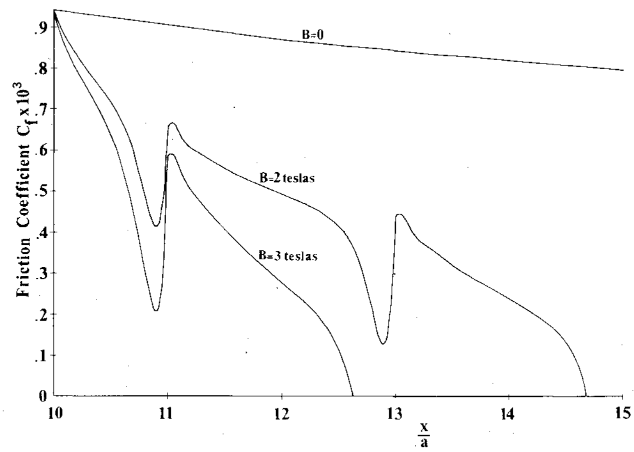

Fig. 4 Variation of friction coefficients and separation points as a function of B for constant area, $u_{\infty i} = 1000$ m/sec. $T_{\infty R} = 2000$ K, $M_{\infty i} = 1.31$; $P_{\infty i} = 1.5\times10^5$ N/m^2; $J_{y\infty} = 12.6$ A/cm^2 and $\sigma_{eff} = 60$ mho/m.

Numerical Results

Computations were carried out leading to laminar boundary-layer separation under a variety of externally imposed conditions. Two different electrical conductivity models were used, as well as different kinds of wall boundary conditions for the solution of the energy equation. In all the calculations, an axial electric field is aplied to suppress the freestream Hall current. Thus the effects of the crossflow phenomenon are reduced due to the absence of the traverse Lorentz force, j_xB in the core flow.

Variations in the freestream properties, in the boundary-layer thickness, and in the friction coefficient for one typical run of cesium seeded argon gas are shown in Fig. 3. The lengths of the conducting and insulating segments, a and b, equal 1 cm and the start of the power section is situated at $x/a = 10$. The freestream reference conditions are: $U_{\infty R} = 1000$ m/sec; $T_{\infty R} = 2000$ K; $P_{\infty R} = 1.5\times10^5$ N/m^2 whereas in the power section $j_{y\infty} = 12.6\times10^4$ A/m^2; $B = 2$ T and $\sigma_{eff} = 60$ mho/m. For this standard run separation occurred over the third electrode segement at $x/a = 14.66$. Eye-catching are the sharp dips of the friction coefficient C_f. These dips are located at the trailing edges of the electrodes (cathodes),

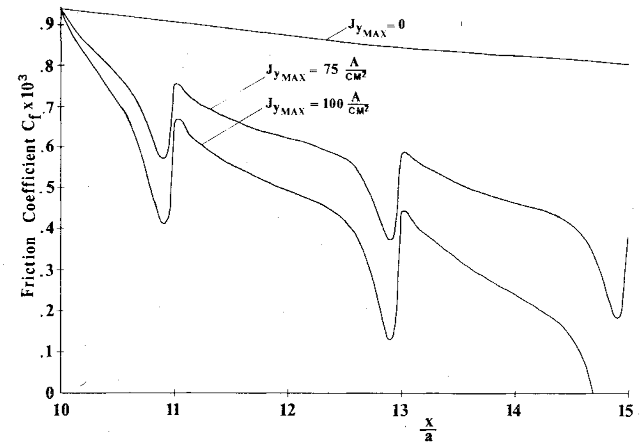

Fig. 5 Variation of friction coefficients and separation points as a function of $J_{y\max}$ with $B=2T$; $\sigma_{\text{eff}}=60$ mho/m; and inlet conditions as in Fig. 4. $J_{y\max}=100$ A/cm^2 gives $J_{y\infty}=12.6$ A/cm^2.

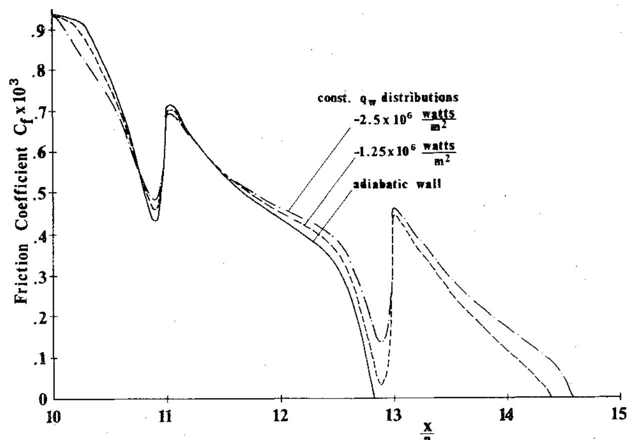

Fig. 7 Variation in friction coefficients and separation points for different values of heat flux q_w with $J_{y\infty}=12.6$ A/cm^2; $B=2$ Torr; $\sigma_{\text{eff}}=60$ mho/m and initial conditions as in Fig. 4.

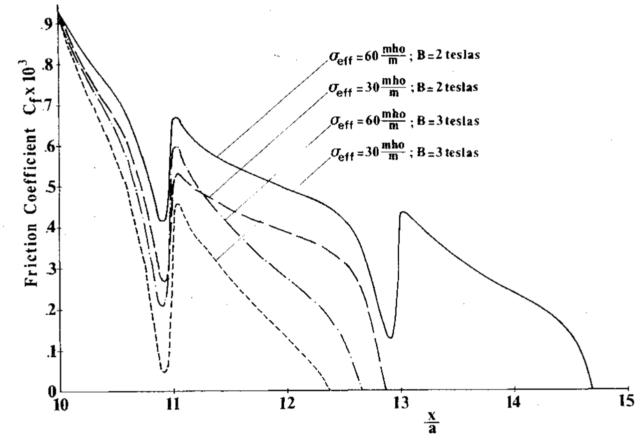

Fig. 6 Variation in friction coefficients and separation points for different values of σ_{eff} with $J_{y\infty}=12.6$ A/cm^2; and inlet conditions as in Fig. 4.

where the current density j_y reaches its maximum value. Here the retarding local Lorentz body forces $j_y\ B_z$ have the highest values, whereas the inertia forces have their lowest values, due to the low gas density resulting from the high local dissipation term $j^2{}_y/\sigma$. The high current density is chosen to avoid excessive computing time in obtaining separation after a relatively short streamwise distance. The same approach was used by one of the authors [15] in small-scale experiments to obtain experimental conditions that could not be achieved otherwise. This does not violate the physical meaning of the results. As a secondary effect sudden increases of the boundary-layer thickness are observed over the regions of high current concentration, with corresponding decreases in the cross-sectional area of the core flow, causing slight dips and bumps in the streamwise variations of the freestream properties. Figures 4 through 6 show the variations in the friction coefficient and separation points for different values of $B, j_{y_{\max}}$ and σ_{eff}. They clearly show the speedy separation for increasing Lorentz body force $j_y B_z$ and increasing overall dissipation $j_y{}^2/\sigma_{\text{eff}}$.

For the calculations presented in the preceding a simplified electrical conductivity model was used, namely the conductivity was assumed to be a constant effective value. Calculations leading to separation were also carried out using the more complicated σ-model Eq. (5). Although the profiles of the dependent variables and the Ohmic heating distributions across the boundary layer were noticeably different, the variations in the friction coefficient and the separation points were almost identical for the two different conductivity models. This is due to the fact that by specifying a fixed wall temperature and thus implying no limit on the heat flux at the wall, the local Ohmic heating within the boundary layer plays a minor role in the near-wall region where the separation process takes place. This result does not agree with the statement made by Alferov et al. [11] who supposed that for fixed wall temperature the Ohmic heating in the boundary layer played a more prominent role.

In general, the wall temperature of an actual generator is not fixed, but the amount of heat conducted through the wall is determined by the thermal conducting property of the duct wall material. For this reason, calculations were also performed when the heat flux at the wall q_w is specified rather than the wall temperature. In Fig. 7, the variations in the shear stress at the wall and the locations of the separation points are presented for different values of q_w. One can see the increased likelihood for separation when the wall is incapable of conducting away the Joule heating generated within the boundary layer. The resulting temperature increase and density decrease in the boundary layer, causing the volumetric Lorentz force to become more influential in the near-wall region, will ultimately lead to an earlier separation.

Finally the relative importance of the electromagnetic effects within the boundary layer on the separation process is estimated. The separation points predicted in Fig. 7 were compared with the results obtained with a purely hypothetical computer experiment where the EM effects are eliminated from within the boundary layer but still retained in the core flow. Excluding the EM effects from the boundary layer eliminated the sharp dips in the skin friction coefficients at the electrode trailing edges and led to the delayed separation. The delays in the separation points, x_s/a, were: for the adiabatic wall from 12.8 to 14.9; for the heat conducting wall at $q_w = -1.25 \times 10^6$ W/m^2 from 14.4 to 15.2 and at $q_w = -2.50 \times 10^6$ W/m^2 from 14.6 to 15.4. Herewith an insight is obtained into the contribution of the boundary-layer electromagnetic effects to the separation process. Of course eliminating the electromagnetic influences from the boundary-layer region but still retaining them in the core region can never be realized in practice. However, such a hypothetical model is useful in the present computer experiment to provide a better understanding of the boundary-layer separation process.

Summary and Conclusion

The separation of supersonic laminar bounday layers from the finite-segmented electrode wall of a Faraday MHD generator has been investigated. Calculations were carried out for a variety of externally imposed conditions, for two different electrical conductivity models, and for different kinds of wall boundary conditions in the solution of the energy equation. A hypothetical model was also used in the present numerical experiment to study the relative importance of the EM effects within the boundary layer in the separation process.

Calculations showed that any variations in the externallly imposed parameters which tend to increase the Ohmic heating in the duct, to increase the magnitude of the axial Lorentz force, or to decrease the inertia of the fluid elements in the near-wall region will favor earlier separation. The strong dependency of separation on the wall temperature and on the heat transfer, which is characteristic of laminar boundary layers in neutral gas, was found to be true also in the separation from the finite-segmented MHD electrode wall.

In the cases where the wall temperature is specified a priori, the contribution to separation by the Ohmic heating within the boundary layer is small compared to the effect of the pressure rise in the core flow. In these cases, the viscosity and the fluid density in the near-wall region, both important parameters on separation, are strongly dictated by the specified wall temperature. For a fixed wall temperature, separation was also found to be independent of the two electrical conductivity models used in the calculations.

In situations where the heat flux at the wall is specified rather than the temperature, calculations showed that Ohmic heating within the boundary layer becomes a more important factor in the separation process. When the duct wall is incapable of conveying away the excsss Joule heating generated within the boundary layer, the resulting increase in temperature and the corresponding decrease in fluid density will bring the Lorentz force to much more prominence, thus favoring the separation process.

The calculation method presented here can be used easily in combination with values for J_y and σ_{eff} found from actual experiments. Modifications are presently being made to the computer program for use in the prediction of turbulent boundary-layer separation from existing MHD generator ducts under actual operating conditions.

References

[1]Hale, F.J. and Kerrebrock, J.L., "Insulator Boundary Layers in Magnetohydrodynamic Channels," *AIAA Journal*, Vol. 2, March 1964, pp. 461-469.

[2]Liubimow, G.A., "The Magnetohydrodynamic Boundary Layers," *Magnitnaya Gidrodinamika*, Vol. 1, No, 3, July 1965, p. 3, English translation.

[3]Lykoudis, P.S., "Transition from Laminar to Turbulent Flow in Magneto-Fluid Mechanic Channels," *Review Modern Physics,* Vol. 32, 1970, p. 796.

[4]Argyropoulos, G.S. et al., "Compressible Turbulent Magnetohydrodynamic Boundary Layers," *The Physics of Fluids*, Vol. 11, No. 12, Dec. 1968, p. 2559.

[5]Ginzburg, I.P. and Skurin, L.I., "The Turbulent Magnetohydrodynamic Boundary Layer in a Compressible Fluid," *Magnitnaya Gidrodinamiks*, Vol. 3, No. 1, 1967, p. 77, English translation.

[6]Sherman, A. et al., "MHD Boundary Layers with Non-Equilibrium Ionization and Finite Rates," AIAA Paper 71-139, New York, 1971.

[7]Cott, D.W., "Ionization and Electron Thermal Nonequilibrium Mangetohydrodynamic Boundary Layers," AIAA Paper 71-138, New York, 1971.

[8]High, M.D. and Felderman, E.J., "Turbulent MHD Boundary Layers with Electron Thermal Nonequilibrium and Finite Rate Ionization," *AIAA Journal*, Vol. 10, Jan. 1972. pp. 98-103.

[9]Doss, E.D., "MHD Boundary Layers on a Segmented Electrode Wall of a Nonequilibrium Generator," Ph.D. thesis, Sept. 1972, Univ. of California at Davis, Davis, Calif.

[10]Teno, J. et al., "Boundary Layers in MHD Generators," Tenth Symposium on Engineering Aspects of Magnetohydrodynamics, Massachusetts Institute of Technology, Cambridge, Mass., March 1969.

[11]Alferov, V.I. et al., "Numercial Experiment Relating to the Detachment of the Laminar Boundary Layer in a Magnetohydrodynamical Channel," *Teplofizika Vysokikh Temperatur*, Vol. 11, No. 3, May 1973, p. 507, English translation.

[12]Patankar, S.V. and Spalding, D.B., *Heat and Mass Transfer in Boundary Layers*, 2nd. ed., Intertext Books, London, 1970.

[13]Cole, D.E. and Hirst, E.A., ed., "Proceedings of the Conference on the Computations of Turbulent Boundary Layers," Vol. II, Dept. of Mechanical Engineering, Stanford University, Stanford, Calif., 1968.

[14]Launder, B.E. and Spalding, D.B., *Lectures in Mathematical Models of Turbulence*, Academic Press Inc. Ltd., London, 1972, p. 32.

[15]Merck, W.F.H., "On the Fully Developed Turbulent Compressible Flow in an MHD Generator," Ph.D. thesis, 1971, Eindhoven University of Technology, Dept. of Electrical Engineering, Eindhoven, the Netherlands.